ACS APPLIED MATERIALS & INTERFACES

Research Article

www.acsami.org

Development of Nanocomposites Reinforced with Carboxylated Poly(ether ether ketone) Grafted to Zinc Oxide with Superior Antibacterial Properties

Ana M. Díez-Pascual*,† and Angel L. Díez-Vicente‡

†Institute of Polymer Science and Technology (ICTP-CSIC), Juan de la Cierva 3, 28006, Madrid, Spain

‡Airbus Operations S. L., John Lennon s/n, 28906, Getafe, Madrid, Spain

ABSTRACT: Novel poly(ether ether ketone) (PEEK) based nanocomposites have been fabricated via melt-blending by addition of a carboxylated polymer derivative covalently grafted onto the surface of hydroxyl-terminated ZnO nanoparticles. Their morphology, thermal, mechanical, tribological, and antibacterial properties have been analyzed and compared with those of composites reinforced with pristine ZnO. The Fourier transform infrared (FT-IR) spectra corroborate the success of the grafting reaction, showing the appearance of signals related to ester linkages. Microscopic observations demonstrate that the polymer grafting improves the nanoparticle dispersion within the matrix. A progressive rise in thermal stability and flame retardant ability is found with increasing ZnO concentration, with an exceptional increment in the maximum degradation rate temperature of 70 °C at 5.0 wt % loading. The crystallization and melting temperature of PEEK decrease upon incorporation of the grafted nanofillers, attributed to the restrictions on polymer chain mobility and crystal growth imposed by the strong ZnO-matrix interactions. Nanocomposites with polymer-grafted nanoparticles exhibit higher stiffness, strength, ductility, toughness and glass transition temperature whilst lower coefficient of friction and wear rate than the neat polymer and composites with bare ZnO. Further, they show superior antibacterial activity against both the Gram-negative *Escherichia coli* and the Gram-positive *Staphylococcus aureus* bacteria. The antimicrobial effect increases upon raising nanoparticle content, and is stronger on *E. coli*. The approach used in this work is a simple, scalable, and efficient method to improve the performance of PEEK/ZnO nanocomposites for use in biomedical applications such as trauma, orthopedics, and spinal implants.

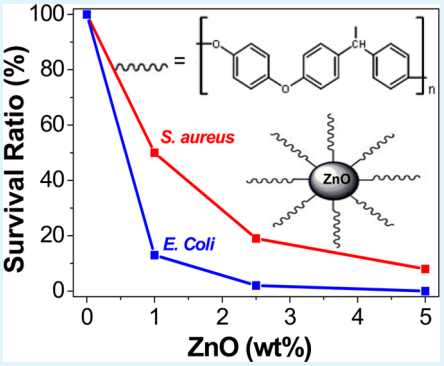

KEYWORDS: *PEEK, ZnO nanoparticles, polymer grafting, mechanical properties, tribology, antibacterial properties*

1. INTRODUCTION

Recently, zinc oxide (ZnO) nanostructures have received much attention within the scientific community owing to their low cost, easy availability, biocompatibility, and possibility of performing surface modifications with different functional groups. They exhibit unique chemical and physical properties including antimicrobial activity, intensive ultraviolet absorption, and high catalytic activity, and therefore are widely used for applications such as solar energy conversion, gas sensors, catalysis, optical devices, and antimicrobials.[1−3] These nanostructures are considered to be nontoxic and generally recognized as safe "GRAS" substances, and recent studies have shown that they do not cause any damage to the DNA of human cells.[4] Moreover, these environmentally friendly nanomaterials have good thermal stability, low coefficient of thermal expansion, high thermal conductivity, and outstanding mechanical properties,[5] and thus are ideal to be employed as reinforcing fillers in polymer composites. In particular, ZnO nanoparticles have been shown to be very effective for decreasing the wear rate of polymers such as polytetrafluoroethylene (PTFE)[6] and ultrahigh-molecular-weight polyethylene (UHMWPE).[7] Many methods have been described in the literature for the preparation of ZnO nanostructures such as laser ablation, hydrothermal synthesis, electrochemical decomposition, thermal evaporation, sonochemical method, sol−gel, anodization, electrophoretic deposition, and so forth.[1,2,8−12] The use of ZnO depends principally on its microstructure, that is, crystallite size, particle size, orientation, and shape. To obtain a proper microstructure, the most challenging is to synthesize small sized particles with few agglomerates and a narrow size distribution.

Poly(ether ether ketone) (PEEK) has emerged as the leading high-performance thermoplastic candidate for replacing metal implant components, especially in orthopaedics and trauma, due to its biocompatibility, inherent chemical resistance, radiolucency, and mechanical properties similar to those of human bones.[13] In addition, it is not cytotoxic, it has good tribological properties, high thermal stability, bioactivity comparable to that of bioinert titanium alloys,[14] and easy processability, and hence it can be shaped by machining and

Received: January 9, 2014
Accepted: February 19, 2014
Published: February 19, 2014

   dx.doi.org/10.1021/am500171x | ACS Appl. Mater. Interfaces 2014, 6, 3729−3741

Scheme 1. Schematic Representation of the Grafting Process of PEEK−COOH onto the Surface of ZnO Nanoparticles

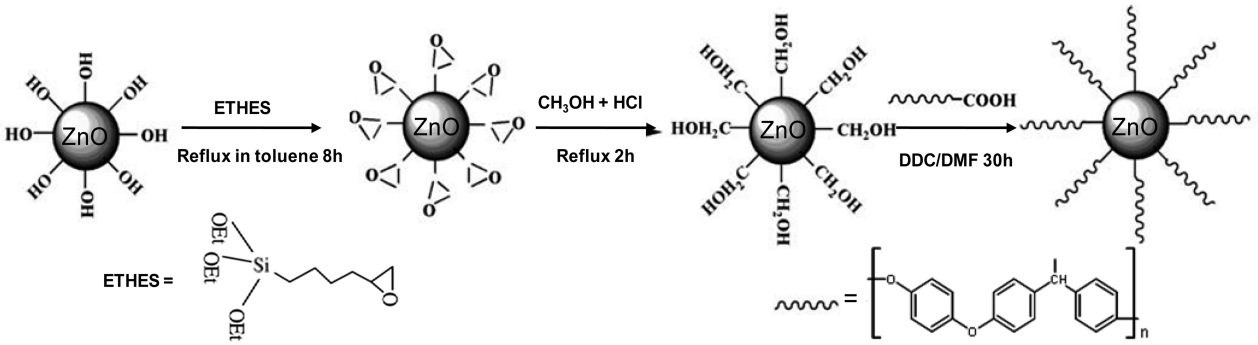

heat contouring to fit the shape of bones.[15] To further improve implant fixation, PEEK biomaterials research has focused on the compatibility of the polymer with bioactive materials, including hydroxyapatite (HA),[16,17] albeit the mechanical properties of these composites are compromised due to poor PEEK−HA physical bonding. Therefore, recent interest has grown in developing PEEK composites reinforced with nanoparticles due to the unique properties arising from their nanoscale structure.[18] The nanoparticles exhibit very high specific surface area that results in the formation of a large interface, hence strong interaction with the polymer matrix. The nanoparticle selection depends on the target properties of the nanocomposite (thermal, mechanical, tribological, optical, magnetic, antimicrobial, etc.). In this regard, different inorganic nanoparticles including silica (SiO_2),[19,20] metal oxides (Al_2O_3, TiO_2, ZrO_2),[21−23] silicon carbide (SiC),[24] silicon nitride (Si_3N_4),[25] and transition metal chalcogenides (WS_2)[26] have been successfully incorporated in PEEK. However, to the best of our knowledge, there is no previous work dealing with the manufacture and characterization of ZnO-reinforced PEEK nanocomposites.

It is well-known that the successful development of polymer nanocomposites depends to a large extent on the ability to uniformly disperse the nanofiller inside the polymer and to achieve a good filler−matrix interfacial adhesion. However, this is frequently a difficult task since nanoparticles have strong tendency to form agglomerates. Further, there is generally poor compatibility between the hydrophobic polymer and the hydrophilic nanofillers. Surface modification of nanoparticles either by chemical or physical methods is a common strategy to enhance the interactions between the organic and inorganic phases.[27] Chemical methods involve modification with coupling agents such as silanes, while physical routes use surfactants or molecules with polar groups that adsorb onto the particle surface via electrostatic interactions. Grafting polymer chains to nanoparticles is another effective way to bring about tunable interfacial interactions in the nanocomposites. Two main approaches have been reported to chemically attach polymeric segments to a filler surface:[28] the covalent bonding of end-functionalized polymers ("grafting to" strategy) and the in situ polymerization with monomer growth of polymer chains from immobilized initiators ("grafting from" method). PEEK is insoluble in the majority of organic solvents, which makes its functionalization difficult;[29] hence, very few works have been reported on the covalent anchoring of PEEK derivatives to nanofillers via the "grafting to" approach.[30,31] Most of the studies carried out the in situ electrophilic grafting of phenoxybenzoic acid monomers onto the filler surface by Friedel-Crafts acylation in polyphosphoric acid.[32,33] Nevertheless, the aromatic electrophilic substitution method is difficult to scale up, and specific monomers must be used to obtain high molecular weight polymers.

The present study reports the covalent attachment of a carboxylated PEEK derivative (PEEK−COOH) onto the surface of hydroxyl-terminated ZnO nanoparticles (ZnO−CH_2OH) via direct esterification reaction under mild conditions (see Scheme 1). For this purpose, the polymer derivative was synthesized through carbonyl reduction followed by addition of glycine amino acid. Moreover, alkyl-hydroxyl groups were introduced onto the surface of ZnO nanoparticles by reaction with 5,6-epoxyhexyltriethoxysilane (EHTES) and subsequent reflux in methanol solution of hydrochloric acid. Different amounts of the resulting PEEK−CO−O−CH_2−ZnO sample have been incorporated as fillers in a PEEK matrix through melt-blending, a simple processing technique that is easy to scale up. For comparative purposes, composites including similar contents of raw ZnO nanoparticles have also been prepared following the same approach. An extensive characterization has been carried out to investigate the morphology, thermal, mechanical, tribological and antibacterial properties of these new nanocomposites suitable for biomedical applications.

2. EXPERIMENTAL SECTION

Materials. PEEK 150P was provided as a coarse powder by Victrex plc, U.K. This low viscosity grade has the following physical characteristics: T_g = 147 °C, T_m = 345 °C, $d_{25°C}$ = 1.32 g/cm^3, $\eta_{350°C}$ = 10^3 Pa·s. The polymer was ground with a ball mill in order to reduce the particle size, vacuum dried at 120 °C for 4 h, and stored in a dry environment. ZnO nanopowder, with <100 nm particle size and specific surface area in the range of 15−25 m^2/g, was supplied by Sigma-Aldrich. 5,6-Epoxyhexyltriethoxysilane (EHTES) was purchased from Gelest, Inc. Dimethyl sulfoxide (DMSO, 99%) and dimethylformamide (DMF, 99%), obtained from Aldrich, were distilled under vacuum and then dried for a few days with a Merck 4 Å molecular sieve. Sodium borohydride ($NaBH_4$), *N*,*N*-dicyclohexylcarbodiimide (DCC, 99%), 4-dimethylaminopyrydine (DMAP, 99%), acetic acid (AcH, 99%), glycine (98.5%), and all the other reagents were also obtained from Sigma-Aldrich and used as received.

Preparation of Hydroxyl-Terminated ZnO (ZnO−CH_2OH). EHTES (3.0 g) was added to a toluene suspension (200 mL) of ZnO (3.0 g) placed in a 250 mL round-bottom flask. The reaction mixture was refluxed at 100 °C for 8 h under a nitrogen atmosphere and magnetic stirring. The resulting material (ZnO−EHTES) was filtered, washed repeatedly with methanol and dried under vacuum at 40 °C for 24 h. The ZnO−EHTES was then refluxed in a methanol solution (300 mL) of hydrochloric acid (1.6 M) at 100 °C for 2 h. In this step, the epoxyhexyl groups were converted into dihydroxyhexyl units.

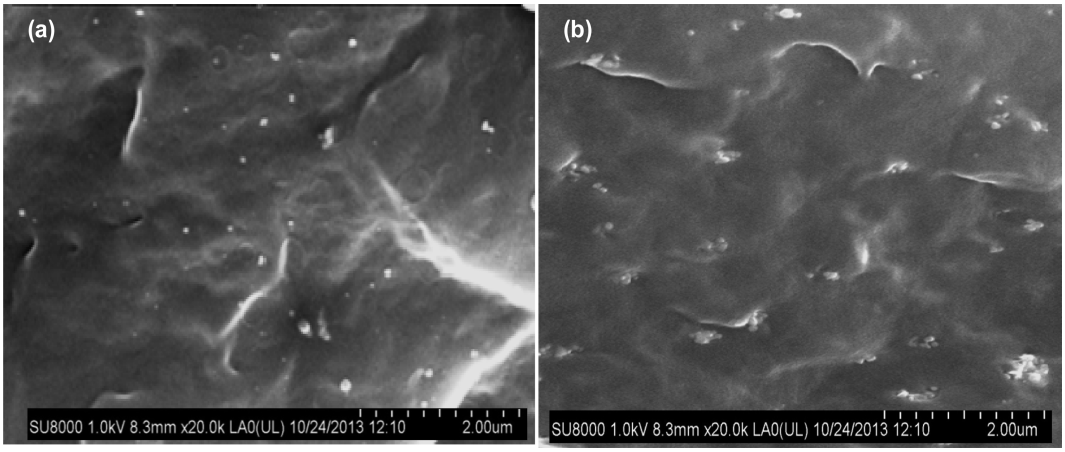

Figure 1. Typical SEM micrographs of PEEK/PEEK−CO−O−CH_2−ZnO (a) and PEEK/ZnO (b) nanocomposites with 2.5 wt % nanoparticle content.

Finally, the resulting solid was washed with methanol thoroughly to remove the unreacted EHTES.

Synthesis of the Carboxylated PEEK Derivative (PEEK−COOH). PEEK (12 g) was slowly added to a stirred solution of $NaBH_4$ (3.6 g) in DMSO (300 mL), and the suspension was heated at 120 °C for 30 h using a thermostat with an ethylene glycol heating liquid. After cooling at room temperature, the suspension was filtered and the solid was washed successively with ethanol, distilled water, and HCl and dried in an oven at 80 °C. The resulting PEEK−OH sample (with ∼45% hydroxylation degree[29] according to thermogravimetric analysis, TGA) was then placed in a 100 mL round-bottom flask and immersed for 72 h at room temperature into a solution of glycine (1.3 g) in AcH (50 mL). Subsequently, it was rinsed successively with AcH, distilled water, and acetone and finally dried in an oven at 80 °C for 3 h. The polymer recovery was about 93 wt %. The functionalization degree of the carboxylated derivative estimated from TGA was ∼29% (see section thermal stability).

Grafting of PEEK−COOH to the Surface of ZnO−CH_2OH. The grafting was carried out via direct esterification through activation of the carboxylic acids of the polymer derivative by carbodiimide (Scheme 1). ZnO−CH_2OH (2.0 g) was dispersed in DMF (60 mL) by ultrasonication for 15 min. Separately, PEEK−COOH (7.0 g) was suspended in DMF (125 mL) and kept at 50 °C for 24 h under stirring. The polymer suspension was added to a solution of DCC (5.1 g) and DMAP (0.4 g) in DMF (250 mL). Then, both polymer and nanoparticle dispersions were mixed and the reaction took place for 30 h at room temperature under mechanical stirring. The resulting solid (PEEK−CO−O−CH_2−ZnO) was filtered, washed with distilled water, methanol and acetone, and finally dried overnight in an oven at 80 °C. The difference between the functionalization degree of PEEK−COOH before and after the esterification reaction corresponds to the extent of the grafting process (∼18% overall degree of grafting; see the Thermal Stability subsection).

Preparation of PEEK Nanocomposites. The PEEK−CO−O−CH_2−ZnO sample was used as a masterbatch to blend with PEEK. The melt-mixing was carried out in a Thermo-Haake MiniLab microextruder at 380 °C, with a rotor speed of 150 rpm during 20 min. Three composites were prepared, with PEEK/PEEK−CO−O−CH_2−ZnO weight ratios of 20/80, 40/60, and 84/16; the effective ZnO content of the nanocomposites is 5.0, 2.5, and 1.0 wt %, respectively. For comparative purposes, composites reinforced with similar amounts of raw ZnO nanoparticles were also prepared under the same processing conditions. After cooling, the samples were pressed into thin films and then annealed for 3 h at 200 °C to increase their crystallinities.

Characterization Techniques. The surface morphology of the nanocomposites was examined by scanning electron microscopy (SEM) with a SU8000 Hitachi scanning electron microscope (Minato-ku, Japan) applying an acceleration voltage of 2.0 kV. Samples were cryo-fractured in liquid nitrogen and then coated with a ∼5 nm Cr overlayer to avoid charge accumulation during electron irradiation.

The attenuated total reflectance Fourier transform infrared (FT-IR) spectra were recorded at room temperature on a Perkin-Elmer Spectrum One spectrometer (PerkinElmer Inc.) equipped with a Universal ATR sampling accessory (diamond crystal) and a red laser excitation source (632.8 nm). four scans were collected for each sample in the wavelength range between 4000 and 400 cm^{-1}. To improve the signal-to-noise ratios, spectra were recorded with an incident laser power of 1 mW and a resolution of 4 cm^{-1}.

The thermal stability of the nanocomposites was analyzed by thermogravimetric analysis (TGA) using a Q50 thermobalance (TA Instruments Ltd., U.K.) at a heating rate of 10 °C/min. Prior to the measurements, samples were dried overnight at 80 °C. The temperature was scanned from room temperature to 800 °C under nitrogen atmosphere. Experiments were carried out on samples with an average mass of 20 mg, with a purge gas flow rate of 60 mL/min.

Dynamic differential scanning calorimetry (DSC) experiments were conducted on a Mettler DSC 30 (Mettler-Toledo, UK) with a TC15 TA controller under a nitrogen atmosphere. Samples with an average mass of 12 mg were melted at 380 °C and kept at this temperature for 5 min to erase the thermal history of the material. Subsequently, they were cooled to 40 °C and reheated to 380 °C, all the steps at a constant rate of 10 °C/min. The transition temperatures were taken as the peak maximum or minimum in the calorimetric curves. The degree of crystallinity of PEEK in the nanocomposites was calculated from the normalized peak enthalpies according to the equation: $X_m = \Delta H_{m,PEEK} / (\Delta H^\circ_{m,PEEK} w_{PEEK})$ where $\Delta H_{m,PEEK}$ is the apparent melting enthalpy of PEEK, w_{PEEK} is the weight fraction of PEEK, and $\Delta H^\circ_{m,PEEK}$ is 130 J/g, the extrapolated value of the enthalpy for a 100% crystalline PEEK sample.[29]

Room temperature X-ray diffractograms were collected with a Bruker D8 Advance diffractometer (Bruker, S.A., Spain) using a Cu tube as X-ray source (λ CuKα = 1.54 Å), with a voltage of 40 kV and an intensity of 40 mA. The results were analyzed with the fitting software Topas 2.1 in Bragg-Brentano geometry in the angular range of 2θ = 5−70°, with an angular increment of 0.05° and an accumulation time of 3 s.

The dynamic mechanical performance was studied using a Mettler DMA861 dynamic mechanical analyzer (Mettler-Toledo, UK). The measurements were carried out in the tensile mode on rectangular shaped bars, in the temperature range between −130 and 250 °C at a heating rate of 2 °C/min and frequencies of 0.1, 1, and 10 Hz. A dynamic force of 6 N was used oscillating at fixed frequency and amplitude of 30 μm.

Tensile properties were measured with an Instron 4204 mechanical tester (Instron Inc.) at room temperature and 50 ± 5% RH, using a crosshead speed of 1 mm/min and a load cell of 1 kN. Tensile specimens (Type V) were employed, according to UNE-EN ISO 527-

1 standard. All the samples were conditioned for 24 h before the measurements. Five specimens for each type of nanocomposite were tested to check for repeatability.

Pin-on-disk tests were performed on a Microtest MT 400-98 equipment (Microtest, S. A., Spain), using a 6 mm diameter 100Cr6 steel-ball-like pattern slide. Measurements were carried out under a constant load of 5 N at a rotation speed of 375 rpm. The system was placed in an isolated box to control the environment conditions, and the experiments were performed under air at 24 ± 2 °C and 22 ± 2% RH. The wear experienced by the flat substrate was determined through the measurement of the wear-track profile by using a profilometer with a resolution of ∼10 nm. For repeatability, each tribological test was repeated 3 times, and the mean values of friction coefficient and wear rate are reported.

The antibacterial activity of the nanocomposites was tested against two test microorganisms: Gram-positive (G+) *Staphylococcus aureus* (ATCC 12600) and Gram-negative (G−) *Escherichia coli* (ATCC 25922). All the samples were sterilized in an autoclave prior to the tests and then submerged in a 3 day old nutrient broth of ∼2.0×10^6 colony forming units per milliliter (CFU/mL). After incubation at 37 °C for 24 h, the number of viable microorganism colonies was counted manually using a pen and a click-counter, and the results were expressed as mean CFU/sample. The survival ratio (SR) was calculated using the equation: SR = $(N/N_0) \times 100$, where N_0 and N are the mean number of bacteria on the pure PEEK and the nanocomposites, respectively. The tests were conducted in triplicate, and the average values are reported.

3. RESULTS AND DISCUSSION

Morphology of the Nanocomposites. The surface morphology of the nanocomposites was examined by SEM, and representative micrographs of samples loaded with an effective ZnO content of 2.5 wt % are shown in Figure 1. The white dots in the images correspond to the nanoparticles. Well dispersed quasi-spherical nanofillers with an average diameter of 80 nm can be visualized in the sample incorporating the carboxylated derivative grafted to the modified ZnO (Figure 1a), while that filled with raw ZnO shows small clusters composed of several particles with a mean size of 60 nm (Figure 1b). The larger nanoparticle size found for PEEK/PEEK−CO−O−CH_2−ZnO is probably ascribed to the presence of polymer chains grafted onto the ZnO surface, pointing towards the success of the esterification reaction. More importantly, the grafting process induced disaggregation of the nanoparticles within the matrix, thus resulting in larger effective contact area between the matrix and filler phases. In addition, the grafting reaction changed the hydrophilicity of the nanoparticles, making them more hydrophobic, thereby promoting their interfacial adhesion with the polymer matrix. Overall, the silane treatment combined with the covalent anchoring of the carboxylated derivative reduced the number of nanoparticle agglomerates and improved their compatibility with the matrix, facts that are critical to improve the mechanical and tribological performance of the nanocomposites.

FT-IR Analysis. The ATR-FTIR spectra of PEEK, the carboxylated derivative, PEEK−CO−O−CH_2−ZnO, raw and modified ZnO as well as the different nanocomposites were recorded to corroborate the success of the esterification reaction and obtain information about the structural changes originated during the different steps of the grafting process (Figure 2). In the spectrum of raw ZnO, a broad peak can be observed at ∼3420 cm^{-1} arising from the OH groups on the nanoparticle surface. Further, an intense peak appears at 440 cm^{-1} that corresponds to the stretching of Zn−O bonds.[34] The spectrum of hydroxyl-terminated ZnO reveals some new peaks

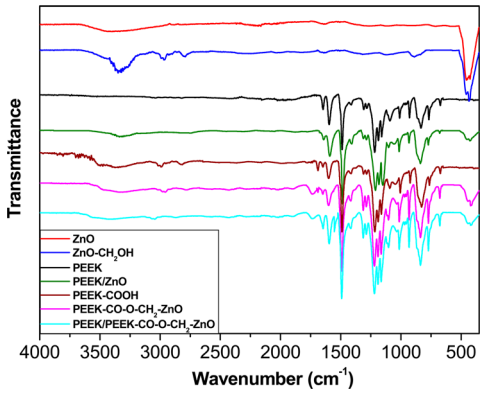

Figure 2. FT-IR spectra of raw and modified ZnO, neat PEEK, PEEK−COOH, PEEK−CO−O−CH_2−ZnO, as well as PEEK/ZnO and PEEK/PEEK−CO−O−CH_2−ZnO nanocomposites with 5.0 wt % effective nanoparticle content.

compared to those of pristine nanoparticles. The bands at 2970 and 2820 cm^{-1} are assigned to symmetrical and asymmetrical C−H stretching vibrations in $-CH_3$ and $-CH_2$ groups, respectively. Furthermore, the peak at 1047 cm^{-1} can be attributed to the Si−O−Si asymmetric stretching, and that at 876 cm^{-1} is assigned to Zn−O−Si symmetrical stretching vibrations.[35] The appearance of these bands proves that the functional groups of EHTES were effectively attached onto the ZnO surface. In addition, the intensity of the peak related to the OH moieties is considerably stronger compared to that of raw nanoparticles, and the maximum is shifted to lower wavenumber, thus corroborating the incorporation of terminal OH groups that interact via H-bonding.

Neat PEEK shows a characteristic peak at 1651 cm^{-1} corresponding to the stretching of the carbonyl group of the benzophenone segment.[36] The intensity of this peak decreases significantly in the case of PEEK−COOH, and simultaneously appears a new signal at around 1700 cm^{-1} that corresponds to the carbonyl stretching of the carboxylic acid.[35] Furthermore, a broad band centred at 3360 cm^{-1} can be observed in the spectrum of the carboxylated derivative, attributed to the stretching vibration of OH groups. All these facts corroborate the successful synthesis of the polymer derivative. The spectrum of PEEK−CO−O−CH_2−ZnO shows some interesting features: a very weak band at 1700 cm^{-1} and a new peak at ∼1738 cm^{-1}, which is characteristically assigned to the C═O stretching of the ester group.[35] This confirms that part of the carboxylic groups of the polymer derivative have reacted with the hydroxyl groups of the silane treated nanoparticles. Moreover, the peak assigned to the stretching of hydroxyl groups appears at lower wavenumber compared to that of the nanoparticles, indicative of the formation of H-bonds. The aforementioned observations corroborate that the grafted sample used as a masterbatch to blend with PEEK is a heterogeneous mixture composed of polymer chains covalently attached to the surface of the ZnO and non-reacted PEEK−COOH segments interacting through polar interactions and H-bonds with the hydroxyl groups of the modified particles.

The spectra of PEEK/ZnO and PEEK/PEEK−CO−O−CH_2−ZnO nanocomposites with 5.0 wt % effective nanoparticle loading are also shown in Figure 2. Very similar spectra were recorded for the rest of the nanocomposites. The spectrum of these samples resembles that of neat PEEK and PEEK−CO−O−CH_2−ZnO, respectively, albeit exhibits an

additional peak at 430 or 422 cm^{-1} (for composites with raw or modified nanoparticles, respectively) assigned to the stretching of Zn−O bonds. This band appears at lower wavenumber compared to that of raw ZnO, shift that is indicative of the existence of nanoparticle−matrix interactions, which are stronger in the nanocomposite with covalent bonds. On the other hand, no sign of the peaks of ETHES is observed in the spectrum of PEEK/PEEK−CO−O−CH_2−ZnO, probably due to their overlapping with the PEEK bands. Overall, FTIR measurements indicate that the esterification reaction between the hydroxyl-terminated ZnO and the carboxylated PEEK derivative took place under the selected conditions, and that the polymer chains were covalently attached onto the surface of the nanoparticles.

Thermal Stability. Figure 3 shows representative TGA thermograms under a nitrogen atmosphere of raw and modified

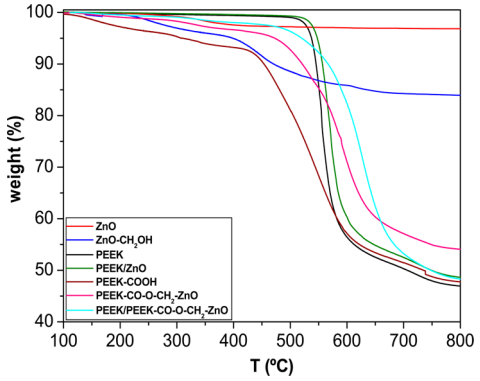

Figure 3. TGA curves under a nitrogen atmosphere of the indicated samples. PEEK/ZnO and PEEK/PEEK−CO−O−CH_2−ZnO nanocomposites contain 2.5 wt % nanoparticle loading.

ZnO, PEEK, the polymer derivative, the grafted sample and the nanocomposites with 2.5 wt % loading. The thermobalance was coupled to a mass spectrometer, enabling the identification of the degradation products. The characteristic degradation temperatures of all the polymeric samples involved in the present study are collected in Table 1. Pristine nanoparticles show a very small weight loss (~2.5 wt %) below 300 °C, probably due to the removal of physically and chemically adsorbed water on their surface. Regarding the hydroxyl-terminated ZnO, two weight losses are detected, one below 300 °C, related to the release of structural water and the decomposition of physically adsorbed ETHES, and the other centred about 470 °C arising from the degradation of the silane coupling agent covalently bonded to the nanoparticles.[37]

Focusing on the thermal stability of the polymeric samples, neat PEEK exhibits a single degradation stage that initiates (T_i) at ~524 °C and shows the maximum rate of weight loss (T_{max}) at 556 °C (Table 1). At 800 °C, the residual mass is about 47% of the initial weight. Analogously, a one step degradation process is observed for the nanocomposites with raw ZnO, although shifted to higher temperatures, demonstrating the thermal stabilization effect caused by the nanoparticles. Thus, T_i increased by 10 and 17 °C, and T_{max} by 15 and 19 °C upon addition of 2.5 and 5.0 wt % ZnO, respectively. On the other hand, three degradation stages can be observed for PEEK−COOH, the first below 260 °C attributed to the splitting-off of the carboxylic moieties, the second in the temperature range between 300 and 390 °C ascribed to the removal of non-oxidized OH groups[29] and the third above 440 °C arising from the decomposition of the main polymer chains.[38] The weight loss of the first step was used to estimate the functionalization degree (~29%) of the carboxylated derivative.

The degradation curve of PEEK−CO−O−CH_2−ZnO also shows three different steps. The stage before 260 °C is associated with the decomposition of the nonreacted carboxylic groups, similar to that found for PEEK−COOH. The second step should be related to the elimination of the nonoxidized hydroxyl groups of the polymer derivative and the decomposition of the coupling agent from the nonreacted modified nanoparticles, while the third stage originates from the degradation of the polymer backbone. Taking into account the weight loss of the first stage, the amount of polymer chains chemically bound to the modified nanoparticles was estimated (within the experimental error). The difference between the functionalization degree of the polymer derivative before and after the esterification reaction corresponds to the extent of the grafting process:[29] ~62% of the COOH groups reacted with the OH moieties of the modified ZnO. Therefore, considering the functionalization degree of the polymer derivative, the overall degree of the grafting procedure is ~18%. It is worthy to note that this grafted sample starts to decompose at a temperature significantly lower than that of PEEK (Table 1), though has higher T_{max} value.

In the case of PEEK/PEEK−CO−O−CH_2−ZnO nanocomposites, three degradation stages are also detected, similar to those described above for the grafted sample. A noticeable

Table 1. Thermal Parameters Obtained from TGA and DSC Analysis of PEEK and the Different Polymeric Samples Prepared in This Work[a]

sample (ZnO content, wt %)	T_i (°C)	T_{10} (°C)	T_{max} (°C)	OI (%)	T_c (°C)	T_m (°C)	X_c (%)
PEEK	524.1	545.7	556.2	36.3	310.6	345.2	42.9
PEEK/ZnO (1.0)	527.3	549.1	564.8	36.7	312.2	345.8	43.2
PEEK/ZnO (2.5)	534.2	556.9	570.9	37.0	318.1	348.3	44.5
PEEK/ZnO (5.0)	541.8	563.4	574.7	38.3	305.6	344.1	41.6
PEEK/COOH	175.1	451.2	547.9	36.6	296.9	337.8	19.6
PCOZnO	313.3	520.4	590.2	39.2	283.5	332.4	7.1
PEEK/PCOZnO (1.0)	413.5	557.8	600.2	36.8	307.2	343.9	41.8
PEEK/PCOZnO (2.5)	404.9	565.9	617.2	37.0	304.9	341.4	38.7
PEEK/PCOZnO (5.0)	387.4	567.2	625.4	38.4	298.6	338.2	34.1

[a]To simplify the nomenclature, PEEK−CO−O−CH_2−ZnO is abbreviated to PCOZnO. T_i, initial degradation temperature obtained at 2% weight loss; T_{10}, temperature for 10% weight loss; T_{max}, temperature of maximum rate of weight loss; OI, oxygen index parameter; T_m, peak melting temperature; T_c, peak crystallization temperature; X_c, degree of crystallinity.

dx.doi.org/10.1021/am500171x | ACS Appl. Mater. Interfaces 2014, 6, 3729−3741

increase in T_{max} is observed compared to that of the neat polymer (Table 1). In particular, this degradation temperature increased by almost 70 °C for the nanocomposite with 5.0 wt % effective ZnO content (about 50 °C rise compared to the composite reinforced with the same amount of raw nanoparticles). Such strong enhancement is attributed to different factors: Firstly, the grafted fillers are better dispersed within the matrix, and effectively hinder the diffusion of the degradation products from the bulk of the polymer to the gas phase, hence slowing down the decomposition process. Secondly, they form covalent bonds with the PEEK−COOH segments, which strongly restrict the mobility of the polymer chains, consequently increasing the barrier effect. Likewise, it has been found[28] that the thermal interfacial resistance between the nanoparticles and the polymer decreases in the presence of chemical bonding, leading to an increase in thermal conductivity that facilitates heat dissipation within the composite. With increasing ZnO loading, the barrier effect becomes stronger, and the thermal conductivity rises, resulting in higher T_{max} values. It is important to highlight that the increments in T_{max} obtained upon addition of PEEK−CO−O−CH_2−ZnO are significantly higher than those reported for PEEK composites reinforced with similar amounts of other inorganic nanoparticles such as raw Al_2O_3, SiO_2, Si_3N_4, and stearic acid-modified SiO_2.[18]

The nanoparticles not only boost the thermal stability of the matrix, but also promote stable char formation, and hence improve the flame retardant ability of the nanocomposites, which can be estimated through the oxygen index (OI). The limiting OI is defined as the minimum amount of oxygen needed in a nitrogen−oxygen mixture (air) to maintain combustion after ignition. This parameter can be easily calculated from the TGA char residues under inert atmosphere through the empirical equation developed by van Krevelen:[39] OI × 100 = 17.5 + 0.4CR, where CR is the char residue in wt % at 800 °C. A material is considered flammable when OI ≤ 26%. Because of its aromatic backbone, PEEK has low flammability (OI = 36.3%) and when burning gives off low levels of smoke and toxic gas. The addition of both raw and modified ZnO improves the fire performance of this polymer, leading to an OI value of 38.4% at 5.0 wt % (Table 1). These enhancements should be related to the higher thermal conductivity of ZnO[40] compared to that of PEEK; thus, the nanoparticles facilitate the rapid dissipation of heat through the bulk of the composite, which means that it takes longer for the surface temperature of the sample to reach the ignition point. Another explanation for this superior flame retardancy could be that the nanoparticles act as an insulator and mass transport barrier that hinder the escape of volatile products generated during the decomposition process and also prevent oxygen from reaching the matrix.

Crystallization and Melting Behavior. The influence of the grafting process on the crystallization and melting behavior of the polymeric nanocomposites was analyzed by DSC. Their crystallization exotherms and heating endotherms are shown in Figure 4, and the calorimetric data derived from DSC analysis are listed in Table 1. The crystallization temperature (T_c) of neat PEEK is about 310 °C. Interestingly, the incorporation of the carboxylic groups leads to a significant decrease in T_c of about 14 °C. Moreover, the level of crystallinity (X_c) of the carboxylated derivative is ∼54% lower than that of PEEK. The substituent groups enable the formation of strong inter and intramolecular hydrogen bonds between the polymeric segments that impose important restrictions on polymer chain

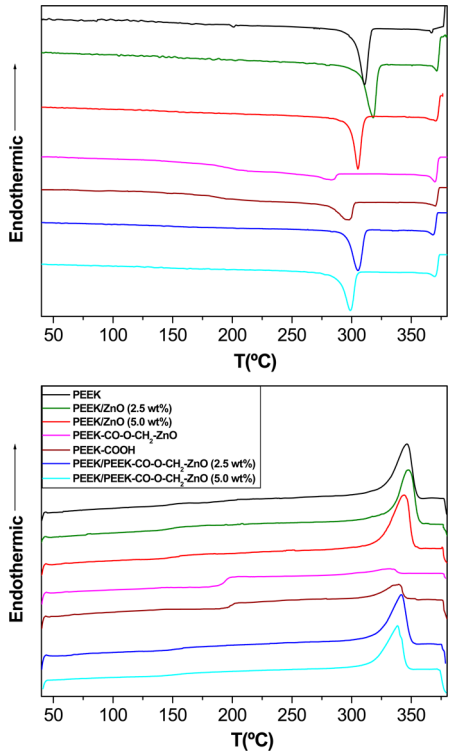

Figure 4. Non-isothermal DSC cooling (top) and heating (bottom) scans at a rate of 10 °C/min.

diffusion and crystal growth, thus slowing down the overall crystallization process, leading to lower X_c and T_c values for the modified polymer. This is in agreement with the results reported for other PEEK derivatives,[29,32] since the substituent groups disrupt the structural regularity and inhibit the molecular packing. In addition, the reduction of the spatial order results in the formation of smaller and less perfect crystals, which have lower melting temperature (T_m), as can be observed from the heating scans (Figure 4, bottom). Regarding the grafted sample, a considerable decrease in all the calorimetric parameters is found compared to those of PEEK−COOH (Table 1), which should be related to the restrictions on mobility arising from the formation of polymer−nanoparticle covalent linkages. Besides, the strong inter- and intramolecular hydrogen bonds between the free carboxylic acids of PEEK−COOH and the nonreacted hydroxyl groups of the modified ZnO also hamper chain diffusion, hence retarding the crystallization of the polymeric segments.

On the other hand, the addition of raw nanoparticles leads to an increase in the T_c, T_m, and X_c of PEEK up to 2.5 wt % loading, whereas at higher concentrations these parameters drop slightly. These facts give hint that when a minor particle content is incorporated in the PEEK matrix, the nucleating effect prevails, whereas at higher loadings the formation of large aggregates hinders the crystal growth, resulting in lower crystallization temperature and crystallinity values. Regarding PEEK/PEEK−CO−O−CH_2−ZnO nanocomposites, a progressive reduction in both transition temperatures and the level of crystallinity is found with increasing nanoparticle content (i.e. around 12 °C in T_c at 5.0 wt % loading, Table 1). Despite that the nanoparticles are homogenously dispersed in these nanocomposites, which would increase the amount of nuclei crystallizing per unit volume of the sample, thus accelerating the nucleation process, the strong interactions between the

composite components (via hydrogen bonding, dipole−dipole and $\pi-\pi$ stacking between the aromatic moieties) probably impede the rearrangement of the macromolecular segments and obstruct the crystal development. Similar inhibitory effect on polymer mobility for crystallization was reported for PEEK nanocomposites incorporating a hydroxylated derivative grafted to single-walled carbon nanotubes (SWCNTs).[31]

Crystalline Structure. The X-ray diffraction patterns of neat PEEK, the carboxylated polymer, pristine and hydroxyl-terminated ZnO, PEEK−CO−O−CH_2−ZnO, and the nanocomposites with 2.5 wt % loading are shown in Figure 5.

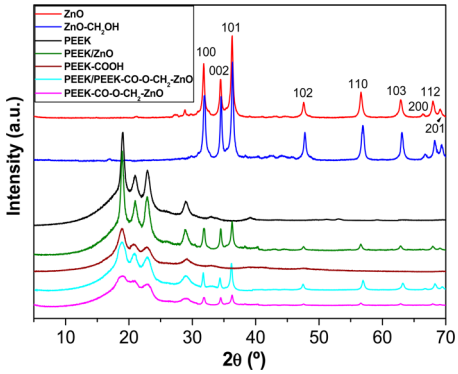

Figure 5. Wide angle X-ray diffractograms at 25 °C. Nomenclature as indicated in Figure 3.

Analogous diffractograms were recorded for the rest of the nanocomposites. The bare nanoparticles show characteristic peaks at 2θ values of 31.8°, 34.4°, 36.2°, 47.6°, 56.6°, 62.9°, 66.4°, and 67.9°, corresponding to the diffraction of the (100), (002), (101), (102), (110), (103), (112), and (201) crystalline planes, respectively. All the diffraction peaks are well indexed to the hexagonal ZnO wurtzite structure (JCPDS data No. 36-1451). Well-defined diffraction peaks and no sign of impurities are detected, confirming the high purity of the nanoparticles. The hydroxyl-terminated particles exhibit very similar pattern to that of pristine ZnO, differing mainly in the intensity and width of some peaks. This corroborates that the silane treatment does not influence the crystalline structure. Further, the average crystallite size of raw and modified ZnO is also comparable (~31 and 28 nm, respectively), as estimated from the full-width at half maximum (FWHM) of the 100, 002, and 101 diffraction peaks using the Scherrer equation.[41]

On the other hand, the diffractogram of neat PEEK shows four main peaks at 2θ values of 18.8°, 20.7°, 22.9° and 28.9°, which correspond to the reflection of the (110), (111), (200), and (211) crystalline planes, respectively, of the orthorhombic unit cell.[38] The polymer derivative shows similar diffractogram to that of the parent polymer, although the peaks are less intense and broader, indicating less structural order induced by the random distribution of the carboxylic groups. However, no shift in the position of the crystalline reflections is observed, hinting that the substituent groups are not included in the crystal unit cell of the modified polymer. The diffractogram of PEEK−CO−O−CH_2−ZnO exhibits the characteristic crystalline reflections of PEEK and ZnO, pointing that the crystalline structure of both sample components is maintained; however, the peaks arising from the polymeric constituent are wider and less intense in comparison to those of the polymer derivative, consistent with the decrease in the level of crystallinity revealed by DSC analysis. Qualitatively similar diffraction pattern is also found for PEEK/ZnO and PEEK/PEEK−CO−O−CH_2−ZnO nanocomposites. Nevertheless, the former composite displays narrower and more intense reflections than the neat matrix, while that including grafted nanofillers shows wider maxima. Thus, the crystal size obtained from the (110) plane of PEEK is 22.1 nm, and decreases by about 25% for the composite incorporating PEEK−CO−O−CH_2−ZnO, whereas for that filled with pristine nanoparticles rises by ~14%. This suggests that the grafted fillers impose a remarkable confinement on the crystal growth, whilst the bare nanoparticles act as nucleating agents and favor the enlargement of the matrix crystals, in agreement with the results from DSC experiments. The grafting of the polymer derivative to the modified nanoparticles leads to a remarkable diminution in the level of crystallinity and to the formation of smaller and less perfect room temperature crystals, facts that are expected to improve the processability of these composites and their blending ability with other materials.

Dynamic Mechanical Analysis. The influence of pristine and polymer-grafted ZnO nanoparticles on the mechanical properties of the composites was explored by DMA. Figure 6

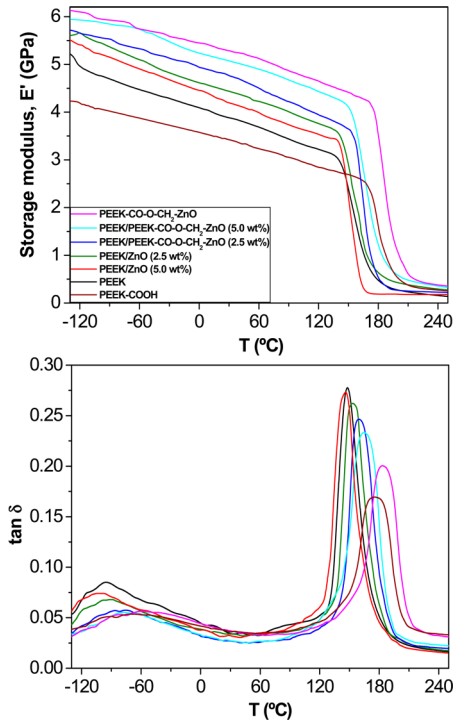

Figure 6. Storage modulus E' (top) and tan δ (bottom) as a function of temperature for the indicated samples.

shows the temperature dependence of the storage modulus (E') and loss factor (tan δ) for neat PEEK and the different nanocomposites studied in this work at the frequency of 1 Hz. DMA data at different temperatures are collected in Table 2. At room temperature, E' of PEEK is about 3.9 GPa and decreases by ~13% for the derivative incorporating carboxylic groups. This behavior may be related to the strong reduction in the level of crystallinity of the derivative, since the crystalline regions enhance the modulus of the semicrystalline polymers. However, the covalent attachment to ZnO results in an exceptional E' increment (~56% compared to that of PEEK−COOH), attributed to a very efficient load transfer from the polymer to the nanoparticles due to the strong interfacial adhesion achieved through the covalent bonding.

dx.doi.org/10.1021/am500171x | ACS Appl. Mater. Interfaces 2014, 6, 3729−3741

Table 2. Data Obtained from DMA Measurements at the Frequency of 1 Hz[a]

sample (ZnO content, wt %)	T_g (°C)	$E'_{-100°C}$ (GPa)	$E'_{25°C}$ (GPa)	$E'_{200°C}$ (GPa)	tan δ_{max} (a.u.)	FWHM (°C)	tan δ_{area} (a.u.)
PEEK	148.0	4.76	3.91	0.22	0.275	23.1	10.1
PEEK/ZnO (1.0)	149.2	5.04	4.11	0.24	0.269	23.4	9.4
PEEK/ZnO (2.5)	152.3	5.41	4.38	0.35	0.263	22.7	8.5
PEEK/ZnO (5.0)	147.1	5.22	4.19	0.18	0.272	23.0	9.9
PEEK/COOH	176.7	4.05	3.42	0.34	0.169	33.6	9.2
PCOZnO	184.5	5.95	5.31	0.58	0.203	30.8	10.5
PEEK/PCOZnO (1.0)	153.7	5.47	4.59	0.43	0.260	25.2	10.9
PEEK/PCOZnO (2.5)	160.6	5.62	4.78	0.48	0.245	27.3	11.6
PEEK/PCOZnO (5.0)	165.4	5.87	5.15	0.31	0.234	28.5	12.0

[a] E', storage modulus; T_g, glass transition temperature; tan δ_{max}, tan δ maximum value; FWHM, full-width at half maximum of the tan δ peak; tan δ_{area}, area under the tan δ peak.

Regarding PEEK/PEEK−CO−O−CH_2−ZnO nanocomposites, a progressive rise in E' is found with increasing nanoparticle content, by up to 32% at 5.0 wt % effective loading in comparison with that of PEEK, pointing out the strong stiffening effect of these grafted nanofillers. In contrast, the inclusion of similar amounts of raw ZnO resulted in smaller increases in the matrix modulus (Table 2), the highest increment being ∼12% at 2.5 wt % loading. Despite that the composites filled with polymer-grafted nanoparticles have lower degree of crystallinity than their counterparts reinforced with bare ZnO, their higher E' values should be related to the more homogenous nanofiller dispersion, as revealed by SEM, combined with a stronger filler−matrix interfacial adhesion due to the presence of the polymer derivative that acts as a compatibilizing agent. Thus, PEEK−COOH can interact both with the nanoparticles via covalent and hydrogen bonding as well as with the matrix via polar interactions and $\pi-\pi$ stacking, and these interactions rule the compatibilizing effect. Moreover, the structural similarity between the derivative and the parent polymer ensures full compatibility of the nanoparticles with the matrix. Regarding nanocomposites with raw nanoparticles, significant aggregates are found at concentrations >2.5 wt %, which have detrimental effects on the mechanical properties. At temperatures above the glass transition, the differences between E' of each composite and the matrix are considerably more significant, indicating that the reinforcing effect of these nanoparticles is more pronounced above the softening point of the matrix. This behavior is in contrast to the results reported for PEEK/SWCNT nanocomposites compatibilized with polysulfones,[42] which revealed higher increase in stiffness below the glass transition. This contradiction could be explained based on aspect ratio and modulus differences between the two types of nanofillers.

The plot of the tan δ (ratio of the loss to storage modulus) as a function of temperature for PEEK and the nanocomposites shows two relaxation peaks:[38] a broad one at low temperatures (around −95 °C for neat PEEK), named β relaxation, associated with local motions of the ketone groups, and an intense maximum at high temperatures (∼148 °C for PEEK), known as α relaxation, which corresponds to the glass transition temperature (T_g). It can be observed from Figure 6 that T_g of the derivative is significantly higher than that of the parent polymer (almost 30 °C, Table 2). Since the glass transition is associated with the mobility of chain segments in the amorphous regions, a plausible explanation is the increment in the energy between adjacent chains caused by intermolecular interactions between the polar groups, mainly via hydrogen bonds. The formation of a strong supramolecular arrangement of the chains decreases the mobility and flexibility of the ether groups, thereby increasing their barriers of bond rotations, leading to such strong T_g increment. Qualitatively similar behavior has also been reported for sulphonated PEEK derivatives, explained in terms of interactions between the sulphonic groups via the ionomer effect.[43] Moreover, the covalent attachment to ZnO produces additional constraints on the mobility of the polymer chains, resulting in further T_g increment (about 8 °C compared to that of PEEK−COOH, Table 2).

With regard to the tan δ data for the different composites (Figure 6), it is evident that the incorporation of grafted nanofillers results in a progressive shift of both relaxations to higher temperatures; this confirms that the well dispersed nanoparticles act effectively as a barrier for the movement of the polymer chains. In particular, T_g increased by ∼17 °C for PEEK/PEEK−CO−O−CH_2−ZnO nanocomposite with 5.0 wt % effective loading as compared to that of the neat matrix. Such increase is higher than those previously reported for other PEEK nanocomposites reinforced with inorganic nanoparticles.[18,26] In contrast, the addition of raw ZnO only results in small T_g increments (Table 2), probably related to the agglomeration of the nanoparticles in certain regions of the matrix, leaving the others with very low reinforcement content. In the latter areas, the molecular movements are only partially limited, and therefore the T_g increment is lower than expected. Similar results have been described for PEEK nanocomposites filled with unmodified SiO_2 or Al_2O_3,[18] ascribed to weak nanofiller−matrix interactions.

It is also noteworthy from Figure 6 that the maximum of the tan δ peak is lower for the polymer derivative compared to that of neat PEEK. This reduction in height could arise from the immobilization of the polymer chains caused by the strong interactions between the chains. Further, a broadening of the peak is observed, which might be related to the random distribution of the substituent groups. In the case of PEEK/PEEK−CO−O−CH_2−ZnO nanocomposites, the height decreases with increasing nanoparticle concentration, reflecting the reduction in mobility induced by these nanofillers. It also indicates good nanoparticle−matrix interfacial adhesion, which becomes stronger with increasing ZnO content, hence leading to better stress transfer between the composite phases. Moreover, this fall in the tan δ_{max} value is less pronounced for samples incorporating bare nanoparticles (Table 2), yet another indication of the less effective barrier effect of the agglomerated nanofillers. On the other hand, DMA curves show a broadening of the tan δ peak for the nanocomposites incorporating PEEK−CO−O−CH_2−ZnO, particularly for that

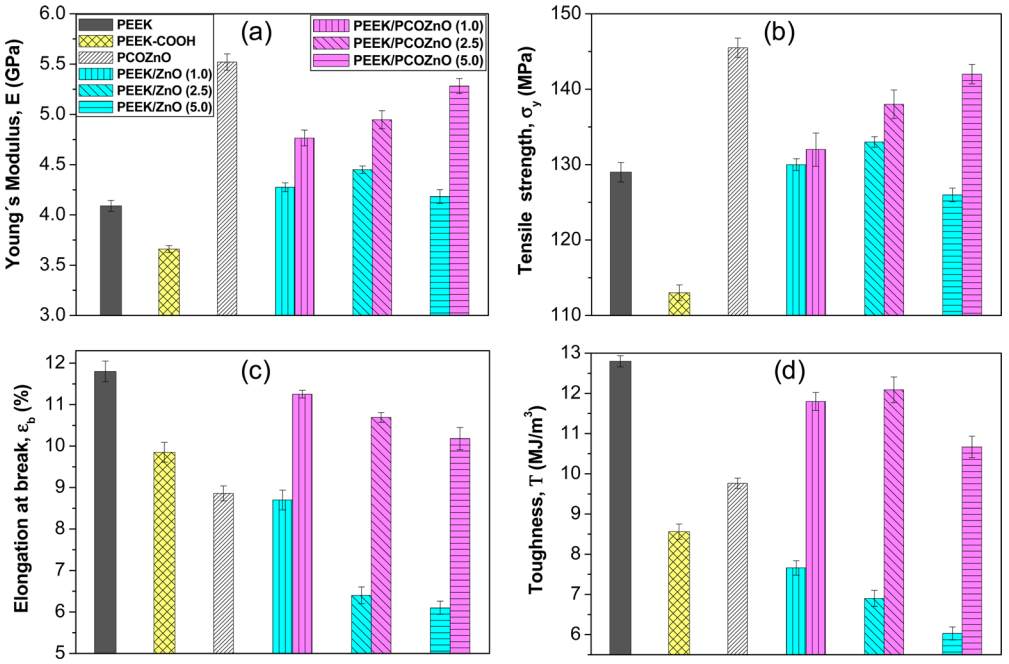

Figure 7. Comparison of the room temperature tensile properties of the different samples: (a) Young's modulus; (b) tensile strength; (c) strain at break; (d) toughness. The values in parentheses indicate the weight percentage of ZnO. To simplify the nomenclature, PEEK−CO−O−CH_2−ZnO is abbreviated to PCOZnO.

with 5.0 wt % loading that shows a FWHM value about 23% higher than that of PEEK (Table 2). This effect could arise from a more heterogeneous amorphous phase in the nanocomposites compared to that of the neat matrix, and has also been interpreted as enhanced nanoparticle−matrix interactions.[26] In contrast, the tan δ peak of composites with raw ZnO is comparable to or even narrower than that of PEEK, reflecting weaker nanofiller−matrix adhesion.

Another interesting parameter derived from DMA curves is the area under the tan δ peak (Table 2), since it is representative of the energy dissipated in the viscoelastic relaxations, hence indicates the impact toughness of the material. It is found that the polymer derivative exhibits smaller area than pure PEEK, while the grafted sample shows higher value, demonstrating that the covalent bonding of the polymer chains to ZnO simultaneously improves the material stiffness and toughness. Composites containing PEEK−CO−O−CH_2−ZnO exhibit larger area than that of the neat polymer, the increase being about 20% for the nanocomposite with 5.0 wt % ZnO; this suggests that the modified nanoparticles improve the matrix ability to dissipate energy. However, for the counterparts incorporating raw ZnO, the area is comparable to or even smaller than that of PEEK. The different behavior found for the two types of composites may be explained considering that the grafting process leads to a more uniform distribution of the nanoparticles, hence less hindrance to the ductile flow of the polymer segments as well as lower stress concentration at the nanofiller−matrix interface. All these effects could help to enhance the material capacity for energy dissipation.

Tensile Properties. The values of Young's modulus (E), tensile strength (σ_y), elongation at break (ε_b), and toughness (T) derived from the stress−strain curves of the different samples are displayed in Figure 7. Neat PEEK shows a Young's modulus of about 4.1 GPa. The incorporation of carboxylic groups results in a 12% reduction of E, probably related to the drop in the level of crystallinity, as discussed previously. Nevertheless, PEEK−CO−O−CH_2−ZnO has higher E than both PEEK and the derivative, in agreement with the results from DMA tests. On the other hand, the addition of low amounts of raw ZnO slightly increases E of PEEK, by up to 9% at 2.5 wt %; however, further rise in the nanoparticle content results in a smaller modulus improvement, probably due to particle agglomeration. In contrast, for the nanocomposites reinforced with grafted fillers, E increases progressively with increasing nanoparticle concentration, showing a maximum augment of 34% at 5.0 wt % loading, attributed to a very efficient reinforcement effect due to the uniform nanoparticle dispersion and the strong adhesion between the matrix and filler phases via covalent and hydrogen bonds as well as polar interactions. It is worthy to note that the improvements in stiffness found upon addition of PEEK−CO−O−CH_2−ZnO to PEEK are higher than those reported for similar composites filled with other unmodified or modified inorganic nanoparticles such as SiO_2 or Al_2O_3,[19−21] demonstrating the suitability of the approach used in this work for developing stiff polymeric composites.

With regard to the tensile strength (Figure 7), the trends observed are qualitatively similar to those described above for the modulus, although the increments compared to that of the pure polymer (∼129 MPa) are smaller, pointing out that polymer-grafted nanoparticles are more effective in enhancing the stiffness than the strength of the matrix. Thus, a maximum increase of ∼10% is found for PEEK/PEEK−CO−O−CH_2−ZnO (5.0 wt %). Again, the raw nanoparticles lead to lower strength increments, due to their poorer dispersion and weaker adhesion to the matrix. On the other hand, the strain at break (about 12% for neat PEEK) drops considerably for the carboxylated derivative, since the strong interactions between the chains obstruct their ductile deformation. The grafted sample also exhibits lower ε_b than PEEK, albeit higher than that of PEEK−COOH. On the other hand, both types of composites show a steady decrease in this parameter with

dx.doi.org/10.1021/am500171x | ACS Appl. Mater. Interfaces 2014, 6, 3729−3741

increasing nanoparticle content; the nanofillers restrict the ductile flow of the polymer segments, which is reflected in lower elongation values. However, the drop in ductility is considerably more pronounced for the composites with raw ZnO, being about 50% for that with 5.0 wt % loading, whereas for the counterpart with grafted nanofillers the fall is only around 13%. The more homogenous nanoparticle dispersion leads to lower stress concentration at the polymer−matrix interface, thus preventing premature failure.

The area under the tensile curve is a measure of the toughness of the system (Figure 7). This parameter is moderately smaller for PEEK−COOH and PEEK−CO−O−CH_2−ZnO in comparison to that of the neat polymer, consistent with the drop in ductility found for these samples. Regarding nanocomposites reinforced with bare ZnO, the toughness decreases gradually as the nanoparticle content rises, with the reduction being ∼53% for the sample loaded with 5.0 wt %. However, for the counterparts incorporating grafted fillers, this area is approximately maintained up to 2.5 wt % ZnO content and then drops slightly (∼15%). For composite materials, the strain at break and toughness tend to be very sensitive to the quality of the dispersion of the filler and its interfacial adhesion with the matrix. In the samples incorporating raw nanoparticles, the small agglomerates likely nucleate the cracks and promote the formation of dimples, aggravating the brittleness of the material during the tensile test. Nevertheless, the grafting of PEEK−COOH onto the modified ZnO improves considerably the toughness of these composites, since helps to maintain the material ability to absorb energy during the deformation process. This behavior is ascribed to a more homogeneous filler dispersion that minimizes the stress concentration nuclei and to an enhanced interfacial adhesion, which can provide an effective barrier for the propagation of cracks.

Tribological Performance. Within the context of the potential use of these nanocomposites as biomaterials for orthopedic, trauma, and spinal implants, it is very important to analyze their tribological performance. As known,[44] inorganic nanoparticles can enhance the tribological properties of polymers, and their effectiveness is conditioned by several factors such as the composite microstructure, filler size and shape, homogeneity of particle distribution, and quality of the filler−matrix interface. Figure 8a compares the mean coefficient of friction (μ) for the different samples studied in this work. The value of μ for neat PEEK and the carboxylated derivative is about 0.35, and decreases significantly (around 50%) upon anchoring the polymer chains onto the surface of the nanoparticles. It has been reported[44] that the covalent grafting causes the immobilization of the nanoparticles in certain positions of the matrix, which prevents their agglomeration at the sliding interface, thereby leading to an effective reduction of the coefficient of friction. Similar beneficial effect on decreasing μ has been reported for epoxy-based composites with grafted nanoparticles such as SiC or Al_2O_3.[45]

Regarding the nanocomposites with bare ZnO, μ drops slightly up to 2.5 wt % loading; however, further increase in the nanoparticle content leads to comparable μ value to that of neat PEEK. This behavior is probably related to the lower stiffness, strength, and toughness found for the composite with higher loading, as revealed by tensile tests, arising from the presence of nanoparticle agglomerates. Bahadur and Sunkara[46] found that ZnO nanoparticles embedded in poly(phenylene sulphide) (PPS), a high-performance thermoplastic similar to PEEK,

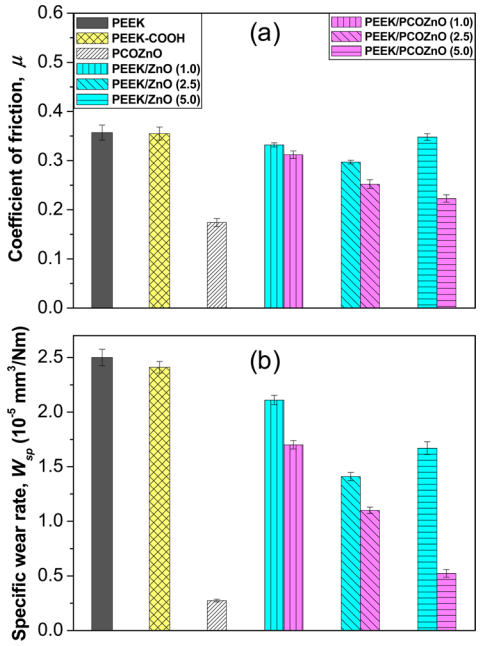

Figure 8. Tribological properties: (a) coefficient of friction; (b) specific wear rate. Nomenclature as indicated in Figure 7.

provoked a rise in μ during sliding against a steel counterface, ascribed to the formation of a discontinuous and poorly bonded transfer film. On the other hand, μ of nanocomposites with PEEK−CO−O−CH_2−ZnO falls gradually with increasing nanoparticle loading, showing a minimum (about 34% drop compared to that of PEEK) at 5.0 wt % ZnO, concentration that corresponds to the maximum improvement in stiffness and strength (Figure 7). This suggests that the presence of well dispersed nanoparticles strongly adhered to the matrix can restrain its scuffing during the sliding process, providing better resistance against the embedding of the hard asperities on the counterpart surface than the neat polymer, which is reflected in lower μ values.

The specific wear rate (W_{sp}) was also determined from the tribological tests (Figure 8b). Neat PEEK and PEEK−COOH show a W_{sp} value of around ∼2.5×10^{-5} mm^3/Nm. The grafting to the modified nanoparticles results in a very strong decrease in this parameter, by about 14-fold drop. This exceptional decrement is again related to the the chemical bonding at the filler−matrix interface, which improves the nanofiller distribution and strengthens the interfacial adhesion between the composite phases. Enhanced wear resistance was previously reported for other composites incorporating polymer-grafted nanoparticles.[44,45] Focusing on nanocomposites filled with pristine ZnO, a moderate decrease in this property is observed, the maximum decrease being about 45% for the composite with 2.5 wt % loading. An analogous trend has been described for ZrO_2 and SiC-reinforced PEEK nanocomposites,[23,24] where W_{sp} passed through a minimum at an optimum nanofiller concentration of ∼2 vol %, attributed to the formation of nanoparticle agglomerates at higher loadings that hamper the development of a continuous transfer film on the counter surface. However, W_{sp} of PEEK/PEEK−CO−O−CH_2−ZnO composites falls gradually upon increasing concentration, and the main drop (∼5.5-fold compared to that of PEEK) corresponds again to the sample with 5.0 wt % ZnO. The stronger increase in wear resistance found for the samples with

grafted nanofillers is ascribed to their improved mechanical properties and nanoparticle dispersion, since a more homogenous filler distribution usually leads to a thinner and more uniform transfer film, facts that result in better tribological properties.[44] Chang and Zhang,[47] working with nano-TiO_2 reinforced epoxy nanocomposites, proposed a rolling mechanism in which the nanoparticles acted as a type of ball-bearing component, meaning that they roll rather than slide between the surfaces, effectively reducing the shear stress, coefficient of friction and contact temperature. Likewise, the nanoparticles served as spacers, preventing the contact between the asperities of the composite surface and the steel counterpart. A similar mechanism could be a suitable explanation for the enhancements in μ and W_{sp} found in this work. It is important to note that PEEK/PEEK−CO−O−CH_2−ZnO nanocomposites exhibit superior tribological performance than PEEK or PPS nanocomposites filled with inorganic nanoparticles such as Al_2O_3, CuO, or ZrO_2, where the coefficient of friction remained comparable to that of the pure matrix, and the wear rate only dropped between 1- and 3-fold.[44]

Antibacterial Properties. Bacterial infections from medical devices are a significant problem because they can persist despite the use of antibiotics, and frequently cannot be eradicated without surgical revision or implant removal, which accounts for a substantial morbidity, and can imply prolonged hospitalization and hence increased health care costs.[48] More importantly, they can even result in amputation or death. Therefore, it is important to evaluate the antibacterial properties of the developed nanocomposites with a view to use them for internal implants.

The antibacterial action of neat PEEK and the nanocomposites was tested against two human pathogen bacteria: *E. coli* (Gram-negative, G−) and *S. aureus* (Gram-positive, G+). As can be observed from Figure 9, the survival ratio of both types of bacteria decreases upon increasing nanoparticle content, with the drop being more prominent at concentrations ≤ 2.5 wt %, and the best antibacterial effect is found for PEEK/PEEK−CO−O−CH_2−ZnO with 5.0 wt % loading. In the concentration range studied, nanocomposites with bare nanoparticles show higher survival ratio, and hence worse antimicrobial effect, compared to the counterparts with polymer-grafted nanofillers, which may be related to their uneven filler dispersion and hence smaller effective surface area. Furthermore, the percentage of variation between the survival ratios for both types of composites increases as the nanoparticle content rises, probably because the differences in the state of nanofiller distribution are more pronounced at higher loadings.

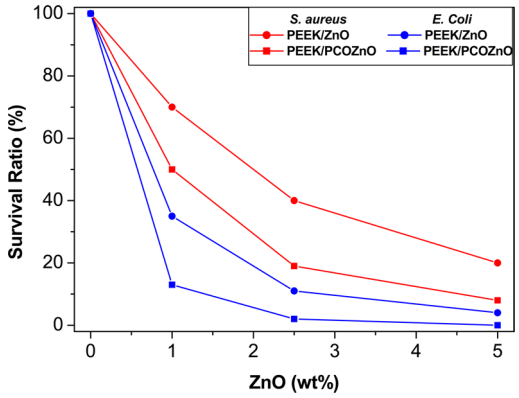

Figure 9. Antibacterial effect of PEEK based composites with different ZnO loadings on the survival ratio of *S. aureus* and *E. coli*. PEEK−CO−O−CH_2−ZnO is abbreviated to PCOZnO.

Figure 9 also shows that the antibacterial effect of both types of composites on *E. coli* is stronger than on *S. aureus*. This is consistent with the study by Liu and Yang,[49] who reported that ZnO is more effective against G− bacteria, and that high nanoparticle loadings in the composites can drastically inhibit the growth of the microorganisms. The different action against these two kinds of bacteria can be ascribed to structural and chemical compositional differences of the cell surfaces.[50] G+ microorganisms usually have one cytoplasmic membrane and a thick wall composed of multilayers of peptidoglycan, while G− ones have a more complex cell wall structure, with a layer of peptidoglycan between the outer membrane and the cytoplasmic membrane. Several mechanisms have been proposed to elucidate the antibacterial activity of these nanoparticles:[50,51] the release of Zn^{2+} ions as a consequence of ZnO decomposition, the mechanical damage of the cell membranes caused by penetration of the nanofillers, and the production of H_2O_2 from the nanoparticle surface. Given that the nanoparticles in PEEK/PEEK−CO−O−CH_2−ZnO nanocomposites are coated by the polymer derivative, the effect of Zn^{2+} release would be restrained. Moreover, the raw and polymer-grafted nanoparticles have mean diameters of 60 and 80 nm, respectively, and thus are not likely to penetrate into the cell wall to harm the bacteria from the interior. Consequently, the production of H_2O_2, a strong oxidizing agent damaging to the cells of living organisms, may be considered as the key factor of the antibacterial activity of these PEEK nanocomposites, and the distinct antimicrobial action towards *S. aureus* and *E. coli* is believed to arise from the different sensitivities towards the H_2O_2 generated. Nonetheless, to verify this hypothesis, an in-depth study of the antibacterial properties of these nanocomposites is necessary, which is out of the scope of this work. Overall, the results obtained reveal the great potential of the developed nanocomposites as antibacterial agents.

4. CONCLUSIONS

In this work, a carboxylated poly(ether ether ketone) derivative (PEEK−COOH) has been covalently anchored onto the surface of hydroxyl-terminated ZnO nanoparticles via direct esterification reaction under mild conditions. Different amounts of the resulting grafted sample have been incorporated as fillers in a PEEK matrix through melt-blending, a simple processing technique easy to scale up. The morphology, thermal, mechanical, tribological, and antibacterial properties of these nanocomposites have been investigated and compared with the behavior of composites directly reinforced with similar contents of pristine ZnO. The FT-IR spectra corroborate the grafting success, showing the appearance of peaks ascribed to ester bonds. SEM micrographs reveal that the polymer grafting minimizes the aggregation of the nanoparticles within the matrix. TGA experiments show a steady increase in thermal stability and flame retardancy upon increasing ZnO concentration, with a rise in the temperature of maximum rate of weight loss up to 70 °C at 5.0 wt % effective loading. DSC thermograms indicate a decrease in the crystallization and melting temperature of PEEK upon addition of polymer-grafted ZnO, since the strong matrix−nanoparticle interactions via covalent and hydrogen bonding hinder the polymer chain mobility and crystal growth. All the nanocomposites exhibit

similar X-ray diffractograms to that of the neat polymer, with the characteristic contribution of the nanoparticles at high diffraction angles. DMA experiments demonstrate a strong increase in both the storage modulus and glass transition temperature of the matrix by the incorporation of grafted nanofillers. Furthermore, the Young's modulus, tensile strength, elongation at break, and toughness of these composites greatly increase whilst the coefficient of friction and wear rate decrease in comparison with those of the neat PEEK and the counterparts reinforced with bare nanoparticles. More importantly, these nanocomposites show superior antibacterial activity against human pathogenic bacteria, the G− *E. coli* and the G+ *S. aureus*. The bactericidal effect is enhanced with increasing nanoparticle content, and the best action is obtained at 5.0 wt % ZnO. This work highlights the great potential of using PEEK/ZnO nanocomposites as biomaterials for orthopedic, trauma, and spinal implants because of their improved mechanical and tribological properties combined with their effective antibacterial action.

AUTHOR INFORMATION

Corresponding Author

*E-mail: adiez@ictp.csic.es.

Notes

The authors declare no competing financial interest.

ACKNOWLEDGMENTS

A.M.D.-P. wishes to acknowledge the Consejo Superior de Investigaciones Científicas (CSIC) for a JAE Postdoctoral Fellowship cofinanced by the EU.

REFERENCES

(1) Sun, Z. P.; Liu, L.; Zhang, L.; Jia, D. Z. Rapid synthesis of ZnO nanorods by one-step, room-temperature, solid-state reaction and their gas-sensing properties. *Nanotechnology* **2006**, *17*, 2266−2270.

(2) Oh, J.-Y.; Lim, S.-C.; Ahn, S. D.; Lee, S. S.; Cho, K.-I.; Koo, J. B.; Choi, R.; Hasan, M. Facile on-step synthesis of magnesium-doped ZnO nanoparticles: optical properties and their device applications. *J. Phys. D: Appl. Phys.* **2013**, *46*, 285101−285107.

(3) Zhang, L.; Jiang, Y.; Ding, Y.; Povey, M.; York, D. Investigation into the antibacterial behavior of suspensions of ZnO nanoparticles (ZnO nanofluids). *J. Nanopart. Res.* **2007**, *9*, 479−489.

(4) Yamada, H.; Suzuki, K.; Koizumi, S. Gene expression profile in human cells exposed to zinc. *J. Toxicol. Sci.* **2007**, *32*, 193−196.

(5) Coleman, V. A.; Jagadish, C. *Basic Properties and Applications of ZnO*; Elsevier: Philadelphia, 2006.

(6) Li, F.; Hu, K.; Li, J.; Zhao, B. The friction and wear of nanometer ZnO filled polytetrafluoroethylene. *Wear* **2001**, *249*, 877−882.

(7) Chang, B. P.; Akil, H. M.; Nasir, R. M.; Nurdijati, S. Abrasive wear performance and antibacterial assessment of untreated and treated ZnO-reinforced polymer composite. *Polym. Compos.* **2013**, *34*, 1020−1032.

(8) Scarisoreanu, N.; Metai, D. G.; Dinescu, G.; Epurescu, G.; Ghica, C.; Nistor, L. C.; Dinescu, M. Properties of ZnO thin films prepared by radio-frequency plasma beam assisted laser ablation. *Appl. Surf. Sci.* **2005**, *247*, 518−525.

(9) Li, F.; Hu, L.; Li, Z.; Huang, X. Influence of temperature on the morphology and luminescence of ZnO micro and nanostructures prepared by CTAB-assisted hydrothermal method. *J. Alloys Compd.* **2008**, *465*, L14−L19.

(10) Rataboul, F.; Nayral, C.; Casanove, M. J.; Maisonnat, A.; Chaudret, B. Synthesis and characterization of monodisperse zinc and zinc oxide nanoparticles from the organometallic precursor [Zn-(C_6H_{11})12]. *J. Organomet. Chem.* **2002**, *643*−*644*, 307−312.

(11) Suwanboon, S.; Amornpitoksuk, P.; Haidoux, A.; Tedenac, J. C. Structural and optical properties of undoped and aluminium doped zinc oxide nanoparticles via precipitation method at low temperature. *J. Alloys Compd.* **2008**, *462*, 335−339.

(12) Ristiac, M.; Musiac, S.; Ivanda, M.; Popoviac, S. Sol−gel synthesis and characterization of nanocrystalline ZnO powders. *J. Alloys Compd.* **2005**, *397*, L1−L4.

(13) Kurtz, S. M.; Devine, J. N. PEEK biomaterials in trauma, orthopedic, and spinal implants. *Biomaterials* **2007**, *28*, 4845−4869.

(14) Sagomonyants, K. B.; Jarman-Smith, M. L.; Devine, J. N.; Aronow, M. S.; Gronowicz, G. A. The in vitro response of human osteoblasts to polyetheretherketone (PEEK) substrates compared to commercially pure titanium. *Biomaterials* **2008**, *29*, 1563−1572.

(15) Barton, A. J.; Sagers, R. D.; Pitt, W. G. Bacterial adhesion to orthopedic implant polymers. *J. Biomed. Mater. Res.* **1996**, *30*, 403−410.

(16) Bakar, A. M. S.; Cheng, M. H. W.; Tang, S. M.; Yu, S. C.; Liao, K.; Tan, C. T.; Khor, K. A.; Cheang, P. Tensile properties, tension-tension fatigue and biological response of polyetheretherketone-hydroxyapatite composites for load-bearing orthopedic implants. *Biomaterials* **2003**, *24*, 2245−2250.

(17) Yu, S.; Hariram, K. P.; Kumar, R.; Cheang, P.; Aik, K. K. In vitro apatite formation and its growth kinetics on hydroxyapatite/polyetheretherketone biocomposites. *Biomaterials* **2005**, *26*, 2343−2352.

(18) Díez-Pascual, A.M.; Naffakh, M.; Marco, C.; Ellis, G.; Gómez-Fatou, M. A. High-performance nanocomposites based on polyetherketones. *Prog. Mater. Sci.* **2012**, *57*, 1106−1190.

(19) Kuo, M. C.; Tsai, C. M.; Huang, J. C.; Chen, M. PEEK composites reinforced by nano-sized SiO_2 and Al_2O_3 particulates. *Mater. Chem. Phys.* **2005**, *90*, 185−195.

(20) Zhang, G.; Schlarb, A. K.; Tria, S.; Elkedim, O. Tensile and tribological behaviors of PEEK/nano-SiO_2 composites compounded using a ball milling technique. *Compos. Sci. Technol.* **2008**, *68*, 3073−3080.

(21) Guoliang, P.; Quiang, G.; Aiguo, T.; Zhiquiang, H. Mechanical behaviors of Al_2O_3 nanoparticles reinforced polyetheretherketone. *Mater. Sci. Eng. A* **2008**, *492*, 383−391.

(22) Chung, C.-J.; Tsou, H.-K.; Chen, H.-L.; Hsieh, P.-Y.; He, J.-L. Low temperature preparation of phase-tunable and antimicrobial titanium dioxide coating on biomedical polymer implants for reducing implant-related infections. *Surf. Coat. Technol.* **2011**, *205*, 5035−5039.

(23) Wang, Q.; Xue, Q.; Liu, H.; Shen, W.; Xu, J. The effect of particle size of nanometer ZrO_2 on the tribological behaviour of PEEK. *Wear* **1996**, *198*, 216−219.

(24) Wang, Q.-H.; Xu, J.; Shen, W.; Xue, Q. The effect of nanometer SiC filler on the tribological behavior of PEEK. *Wear* **1997**, *209*, 316−321.

(25) Balaji, V.; Tiwari, A. N.; Goyal, R. K. Fabrication and properties of high performance PEEK/Si_3N_4 nanocomposites. *J. Appl. Polym. Sci.* **2011**, *119*, 311−318.

(26) Naffakh, M.; Diez-Pascual, A. M.; Marco, C.; Gómez, M. A.; Jiménez, I. Novel melt-processable poly(ether ether ketone)(PEEK)/inorganic fullerene-like WS_2 nanoparticles for critical applications. *J. Phys. Chem. B* **2010**, *114*, 11444−11453.

(27) Kickelbick, G. Concepts for the incorporation of inorganic building blocks into organic polymers on a nanoscale. *Prog. Polym. Sci.* **2003**, *28*, 83−114.

(28) Zou, H.; Wu, S.; Shen, J. Polymer/silica nanocomposites: preparation, characterization, properties, and applications. *Chem. Rev.* **2008**, *108*, 3893−3957.

(29) Diez-Pascual, A. M.; Martínez, G.; Gómez, M. A. Synthesis and characterization of poly(ether ether ketone) derivatives obtained by carbonyl reduction. *Macromolecules* **2009**, *42*, 6885−6892.

(30) Diez-Pascual, A. M.; Martínez, G.; González-Domínguez, J. M.; Martínez, M. T.; Gómez, M. A. Grafting of a hydroxylated poly(ether ether ketone) to the surface of single-walled carbon nanotubes. *J. Mater. Chem.* **2010**, *20*, 8285−8296.

(31) Diez-Pascual, A. M.; Martínez, G.; Martínez, M. T.; Gómez, M. A. Novel nanocomposites reinforced with hydroxylated poly(ether ether ketone)-grafted carbon nanotubes. *J. Mater. Chem.* **2010**, *20*, 8247−8256.
(32) Oh, S. J.; Lee, H. J.; Keum, D. K.; Lee, S. W.; Wang, D. H.; Park, S. Y. *Multiwalled* carbon nanotubes and nanofibers grafted with polyetherketones in mild and viscous *polymeric* acid. *Polymer* **2006**, *47*, 1132−1140.
(33) Jeon, I.-Y.; Tan, L.-S.; Baek, J.-B. Nanocomposites derived from in situ grafting of linear and hyperbranched poly(ether-ketone)s containing flexible oxyethylene spacers onto the surface of multiwalled carbon nanotubes. *J. Polym. Sci., Part A: Polym. Chem.* **2008**, *46*, 3471−3481.
(34) Abdolmaleki, A.; Mallakpour, S.; Borandeh, S. Effect of silane-modified ZnO on morphology and properties of bionanocomposites based on poly(ester-amide) containing tyrosine linkages. *Polym. Bull.* **2012**, *69*, 15−28.
(35) Colthup, N. B.; Day, L. H.; Wiberley, S. E. *Introduction to Infrared and Raman Spectroscopy*, 3rd ed.; Academic Press, Inc: San Diego, 1990.
(36) Ellis, G.; Naffakh, M.; Marco, C.; Hendra, P. H. Fourier transform Raman spectroscopy in the study of technological polymers. Part 1: poly(aryl ether ketones), their composites and blends. *Spectrochim. Acta, Part A* **1997**, *53*, 2279−2294.
(37) He, H.; Duchet, J.; Galy, J.; Gerard, J.-F. Grafting of swelling clay materials with 3-aminopropyltriethoxysilane. *J. Colloid Interface Sci.* **2005**, *288*, 171−176.
(38) Díez-Pascual, A. M.; Naffakh, M.; Gómez, M. A.; Marco, C.; Ellis, G.; Martinez, M. T.; Anson, A.; Gónzalez-Domínguez, J. M.; Martinez-Rubi, Y.; Simard, B.; Ashrafi, B. The influence of a compatibilizer on the thermal and dynamic mechanical properties of PEEK/carbon nanotube composites. *Nanotechnology* **2009**, *20*, 315707−315715.
(39) van Krevelen, D. W. Some basic aspects of flame resistance of *polymeric* materials. *Polymer* **1975**, *16*, 615−620.
(40) Huang, Z. X.; Tang, Z. A.; Yu, J.; Bai, S. Thermal conductivity of nanoscale polycrystalline ZnO thin films. *Phys. B* **2011**, *406*, 811−823.
(41) Alexander, L. E.; Krieger, R. E. *X-ray Diffraction Methods in Polymer Science*; Willey: New York, 1969.
(42) Diez-Pascual, A. M.; Naffakh, M.; Gonzalez-Dominguez, J. M.; Ansón, A.; Martinez-Rubi, Y.; Martinez, M. T.; Simard, B.; Gómez, M. A. High performance PEEK/carbon nanotube composites compatibilized with polysulfones-I. Structure and thermal properties. *Carbon* **2010**, *48*, 3485−3499.
(43) Zaidi, S. M.; Mikhailenko, S. D.; Robertson, G. P.; Guiver, M. D.; Kaliaguine, S. Proton conducting composite membranes from poly ether ether ketone and heteropolyacids for fuel cell applications. *J. Membr. Sci.* **2000**, *173*, 17−34.
(44) Friedrich, K.; Schlarb, A. K. In *Tribology of polymeric nanocomposites*; Briscoe, B. J., Ed.; Tribology and Interface Enginnering Series 55; Elsevier: Oxford, 2008.
(45) Zhang, M. Q.; Rong, M. Z.; Yu, S. L.; Wetzel, B.; Friedrich, K. Improvement of tribological performance of epoxy by the addition of irradiation grafted nano-inorganic particles. *Macromol. Mater. Eng.* **2002**, *287*, 111−115.
(46) Bahadur, S.; Sunkara, C. Effect of transfer film structure, composition and bonding on the tribological behavior of polyphenylene sulfide filled with nano particles of TiO_2, ZnO, CuO, and SiC. *Wear* **2005**, *258*, 1411−1421.
(47) Chang, L.; Zhang, Z. Tribological properties of epoxy nanocomposites: II. A combinative effect of short carbon fiber and nano-TiO_2. *Wear* **2006**, *260*, 869−878.
(48) Knetsch, M. L. W.; Koole, L. H. New strategies in the development of antimicrobial coatings: The example of increasing usage of silver and silver nanoparticles. *Polymers* **2011**, *3*, 340−366.
(49) Liu, H. L.; Yang, T. C. K. Photocatalytic inactivation of *Escherichia coli* and *Lactobacillus helveticus* by ZnO and TiO_2 activated with ultraviolet light. *Process Biochem.* **2003**, *39*, 475−481.
(50) Brayner, R.; Ferrari-Iliou, R.; Brivois, N.; Djediat, S.; Benedetti, M. F.; Fievet, F. Toxicological impact studies based on *Escherichia coli* bacteria in ultrafine ZnO nanoparticles colloidal medium. *Nano Lett.* **2006**, *6*, 866−870.
(51) Heinlaan, M.; Ivask, A.; Blinova, I.; Dubourguier, H. C.; Kahru, A. Toxicity of nanosized and bulk ZnO, CuO and TiO_2 to bacteria *Vibrio fischeri* and crustaceans *Daphnia magna* and *Thamnocephalus platyurus*. *Chemosphere* **2008**, *71*, 1308−1316.